Observation of multi-Raman gain resonances in rubidium vapor*

Jun Liu(刘俊), Dong Wei(卫栋)†, Jin-wen Wang(王金文), Ya Yu(余娅), Hua-jie Hu(胡华杰), Hong Gao(高宏)‡, and Fu-li Li(李福利)

Key Laboratory of Quantum Information and Quantum Optoelectronic Devices of Shanxi Province, School of Science, Xi'an Jiaotong University, Xi'an 710049, *China*

(Received 14 March 2016; revised manuscript received 26 May 2016; published online 28 September 2016)

We present an experimental study of multi-Raman gain resonances in a hot rubidium vapor. The experiment is performed based on a high-efficiency four-wave mixing process due to the Raman-driven coherence in a double-Λ configuration. The Raman gain resonance for ^{85}Rb atoms under a bias magnetic field is shown to be split into five or six peaks, depending on the orientation of the magnetic field. The formed multi-Raman gain resonances have potential applications in measurement of magnetic fields and generation of multi-frequency correlated twin beams.

Keywords: four-wave mixing, multi-Raman gain resonances, coherent optical effects

PACS: 42.50.–p, 42.50.Dv, 42.65.–k **DOI:** 10.1088/1674-1056/25/11/114204

1. Introduction

Quantum coherence and quantum interference can lead to many interesting quantum optical phenomena. A typical phenomenon is the active Raman gain (ARG),[1] which has been widely used to achieve subluminal[2,3] and superluminal propagations,[4] large Kerr nonlinearity,[5] narrow-gain spectrum,[6] and so on. From experimental and theoretical studies, we know that the quantum coherence can be used to enhance the nonlinear susceptibility. The combination of the ARG and the four-wave mixing (FWM) is therefore investigated by many groups. It has been proven that the FWM process assisted by the ARG can amplify the input probe field and produce a phase conjugate field simultaneously. A scheme can also be used to generate bright correlated twin beams,[7–11] which are an important quantum resource for developing practical quantum information protocols.

Recently, a configuration named a N-resonance has been extensively studied.[12–15] The N-resonance can be considered as a type of three-photon, two-optical field absorptive resonance. A scanning probe field is tuned to the Doppler broadened atomic transition between the upper hyperfine level of the ground state and the electronically excited state, and optically pumps the atoms into the lower hyperfine level of the ground state, while the pump field is red detuned from the transition. When the frequency difference between the pump and the probe fields is equal to the hyperfine splitting of the ground state, the established two-photon Raman resonance drives the atoms coherently from the lower hyperfine level to the upper one, thereby inducing an increased absorption of the probe field. In Ref. [16], the authors studied the N-resonance splitting in magnetic fields with cesium atoms. In Ref. [17], the N-resonance splitting in a strong magnetic field was demonstrated with a thin Rb cell. These results can be used to study the behavior of the ground-state levels of alkali atoms[18] in a wide range of magnetic fields. However, due to the existence of the Doppler absorption profile, the signal to noise ratio is low.

In this paper, we present an experimental study of a Raman gain resonance under magnetic fields in a rubidium vapor cell. Our experiment is performed based on a high-efficiency FWM process due to the Raman-driven coherence in a double-Λ configuration. In contrast from the N-resonance experiment, both the pump and the probe beams have large single photon detunings from the atomic transition in our experiment. Thus the measured signal is Doppler-free. Moreover, when two two-photon resonances are established in the double-Λ three-level scheme, we can observe the Raman gain resonance rather than the absorption resonances. Furthermore, we find that the Raman gain resonance can be split into five or six peaks under magnetic fields (for simplicity, we will refer to them as multi Raman gain resonances), which depends on the magnetic field orientation with respect to the laser propagation direction. The experimental results can be used not only for the measurement of magnetic fields but also for the generation of multi-color quantum correlated twin beams.[19]

The organization of the rest of this paper is as follows. In Section 2, we briefly introduce the basic theory and the experimental setup. In Section 3, we show the experimental results and the corresponding explanations. And in Section 4, we conclude the paper.

*Project supported by the National Natural Science Foundation of China (Grant Nos. 11374238, 11574247, and 11534008) and the Fundamental Research Funds for the Central Universities, China (Grant No. xjj2014097).

†Corresponding author. E-mail: weidong@mail.xjtu.edu.cn

‡Corresponding author. E-mail: honggao@mail.xjtu.edu.cn

© 2016 Chinese Physical Society and IOP Publishing Ltd

2. Basic theory and experimental setup

2.1. Basic theory

As shown in Fig. 1, which is a double-Λ configuration formed with rubidium atoms. The energy levels are taken as the following ^{85}Rb D_2 line: $|1\rangle = |5S_{1/2}, F = 2\rangle$, $|2\rangle = |5S_{1/2}, F = 3\rangle$, $|3\rangle = |5P_{3/2}, F'\rangle$. The two transitions from $|1\rangle$ to $|3\rangle$ and from $|2\rangle$ to $|3\rangle$ are simultaneously driven by a strong pump field with different single-photon detunings Δ and $\Delta + \delta$, where δ is the hyperfine splitting of the ground state of ^{85}Rb and Δ is the blue detuning from $|3\rangle$. The transition $|1\rangle$ to $|3\rangle$ is also coupled by a weak probe field with large single-photon detuning $\Delta + \delta$. In this configuration, an atom can be driven to jump back and forth between the two hyperfine ground states. Meanwhile, two pump photons are simultaneously absorbed and converted into one probe photon and one conjugate photon. So the probe light is amplified by a stimulated Raman non-degenerate FWM process, while the conjugate light is generated with frequency $\omega_c = 2\omega_0 - \omega_p$, where ω_0, ω_p, and ω_c, are the angular frequencies of the pump, the probe, and the conjugate beams, respectively. Here, the probe and the conjugate beams share the same pump beam and form a double-Λ configuration. The relative intensity squeezing between the probe and the conjugate beams can also be generated based on this configuration.[7–11]

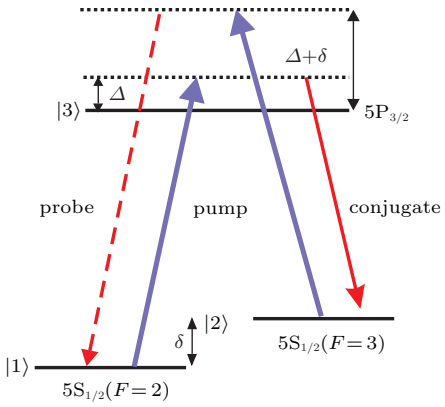


Fig. 1. (color online) Double-Λ scheme of the D_2 line of ^{85}Rb. The energy level configuration is taken as the following: $|1\rangle = |5S_{1/2}, F = 2\rangle$ and $|2\rangle = |5S_{1/2}, F = 3\rangle$ are two ground states of the ^{85}Rb atoms, and $|3\rangle = |5P_{3/2}, F'\rangle$ is the excited state. The hyperfine splitting of the excited state is not resolved compared with our large detuning.

Now let us consider what happens when we apply a bias magnetic field to the Rb atoms. Suppose that the magnetic field is applied longitudinally. From the Zeeman effect, we know each magnetic sublevel $|F, m_F\rangle$ will be shifted by an amount $\mu_B g_F m_F B$, where $\mu_B = 1.4$ MHz/G is the Bohr magneton, g_F is the Lande g factor of the level, and B is the strength of the magnetic field. From the ^{85}Rb data,[17] we know that the splitting of neighboring Zeeman sublevels of $|5S_{1/2}, F = 3\rangle$ and $|5S_{1/2}, F = 2\rangle$ with a moderate bias magnetic field is about 0.467 MHz/G and −0.467 MHz/G. For the longitudinal magnetic field case, the atomic quantization axis is set along the beam propagation direction and a linearly polarized beam will be seen in the atom's frame as two orthogonal circularly polarized beams. The corresponding left- and right-circularly polarized components couple the Zeeman levels of $\Delta m = \pm 1$. According to this interpretation, eight Λ-subsystems can be formed for the two orthogonal circularly polarized pump and probe beams, as shown in Fig. 2. Here, the solid lines represent the pump beam and the dashed lines represent the probe beam. Considering the frequency degenerate case, we can conclude that the Raman-gain resonance will split into five peaks under the longitudinal magnetic field. The similar situation can also be formed with the pump and the conjugate beams. Moreover, two subsystems with $m_F = 0$ in the excited state cause a resonant peak located at the same position as the resonance without a bias magnetic field. While the other transitions symmetrically distribute on two sides. The frequency shift between the neighboring peaks should be 0.934 MHz/G.

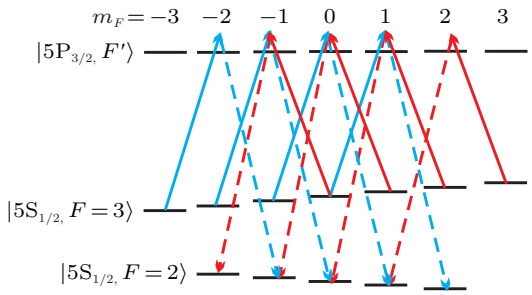


Fig. 2. (color online) Eight Λ-subsystems are formed by orthogonal circularly polarized probe and pump fields in a longitudinal magnetic field. The similar configuration can also be formed by the pump and the conjugate fields.

If the magnetic field is applied transversely, that is to say, the magnetic field is perpendicular to the propagation direction of light, the resonance occurs differently for different configuration corresponding to the direction of the magnetic field and the polarized direction of light. Consider the case where the magnetic field is applied along the polarized direction of the pump beam or perpendicular to the polarized direction of the probe beam, then the pump beam couples the Zeeman levels of $\Delta m = 0$ while the probe beam couples the Zeeman levels of $\Delta m = \pm 1$. They form Λ-systems shown in Fig. 3. A similar situation can also be formed for the pump and the conjugate beams. There exist two kinds of transitions determined by $\Delta m_F = 1$ (black curve) and $\Delta m_F = -1$ (red curve), and then eight subsystems can be formed. Because some of the frequencies are degenerate, there are only six independent resonances left. The six peaks are located symmetrically about the resonance without the bias magnetic field. The frequency difference between the neighboring peaks is also 0.934 MHz/G, which is the same as the splitting in the longitudinal magnetic field.

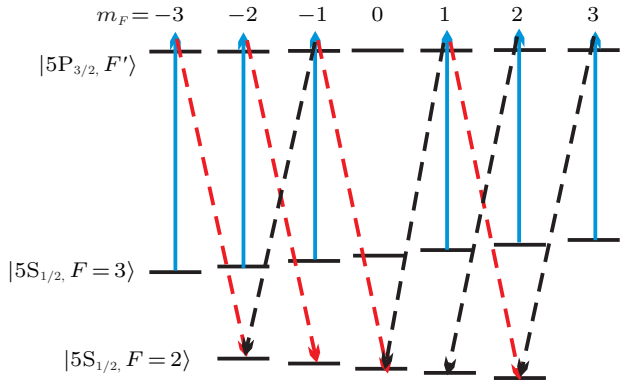


Fig. 3. (color online) Eight Λ-like subsystems are formed by a linearly polarized probe beam and a circularly polarized pump in a transverse magnetic field. The similar configurations can also be formed by the pump and the conjugate fields.

2.2. Experimental setup

Our experimental apparatus is shown in Fig. 4, which consists of two external cavity diode lasers (Toptic DL100) and one tapered amplifier (Toptic, BoostTA). The laser frequency is monitored using a standard saturated absorption spectroscopy (SAS). The pump beam is seeded into the tapered amplifier (TA) to boost the power. After the single mode fiber (SMF), the power of the pump and the probe beams are 450 mW and 200 μW, respectively. We combine the pump and the probe beams with orthogonal linear polarizations on a PBS and send them into an enriched ^{85}Rb vapor cell. The two beams are crossed with an angle less than 0.5° to spatially separate for detection. The cell is 15-mm long and the two windows are anti-reflection coated to reduce reflection losses. The cell is temperature-stabilized at 113 °C with the atomic density of 1.3×10^{13} cm^{-3}.[20] We use a pair of Helmholtz coils to generate a bias magnetic field. After the cell, the pump beam is filtered using another PBS and the probe beam is sent into a photodetector (PD) to record the signal.

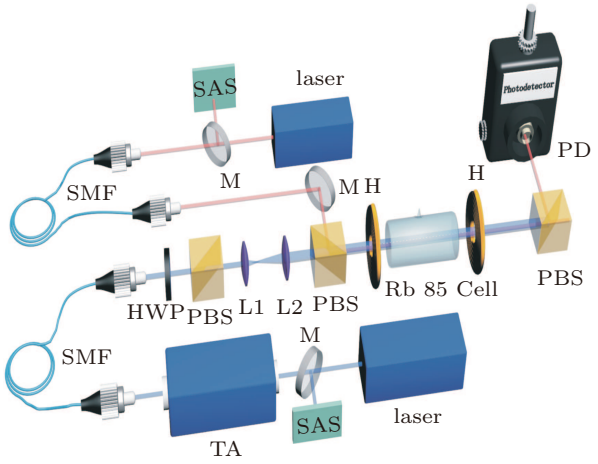


Fig. 4. (color online) The experimental setup. TA, tapered amplifier; M, mirrors; PBS, polarizing beam splitter; HWP, half wave plate; L1, lens; SMF, single mode fiber; H, Helmholtz coil set for longitudinal case; PD, detector; SAS, saturated absorption spectroscopy.

3. Experimental results and discussion

3.1. Multi Raman resonance without a bias magnetic field

In our experiment, the frequency of the probe beam is scanned about 10 GHz across the D_2 line while the pump frequency is fixed. First, let us check the experimental result without a bias magnetic field. Figure 4 shows the transmitted spectroscopy of the probe beam versus the frequency detuning detected by the PD. The pump beam is blue detuned about 900 MHz of ^{85}Rb $|5S_{1/2}, F = 2\rangle \rightarrow |5P_{3/2}\rangle$ as shown in Fig. 5. We can see that there are two probe intensity gain peaks emerged at the red and blue of the pump position. These peaks are caused by the forward FWM gain. The frequency detunings of the two peaks relative to the pump field are equal to the ^{85}Rb ground-state hyperfine splitting, which is approximately 3 GHz. The blue one of the two peaks shows only a gain character but the red one shows a slight dispersive character which is induced by the Raman absorption near the atomic transitions.

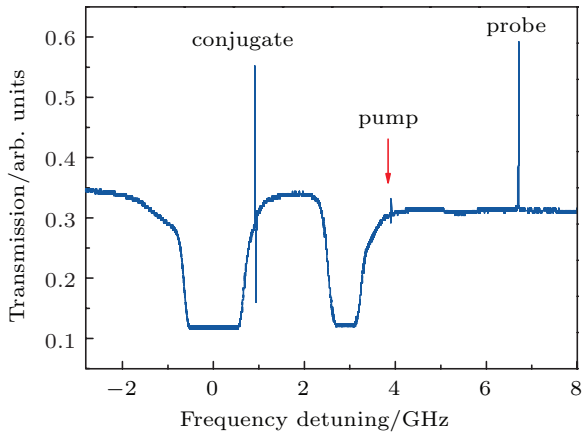


Fig. 5. (color online) Probe transmission versus detuning from the ^{85}Rb transition. The pump beam is blue detuned about 900 MHz of the ^{85}Rb $5S_{1/2}, F = 2 \rightarrow 5P_{3/2}$.

3.2. Multi Raman resonance with a longitudinal magnetic field

Now let us look at the effect of a longitudinal magnetic field applied to the Raman gain resonance. We set up a pair of Helmholtz coils to provide the bias magnetic field. The distance between the center of the Rb cell and the Helmholtz coil is 5 cm, and the magnetic field can be changed from 0 G to 61 G with an adjustable DC power supply. The measured magnetic resolution is 1 G owing to the resolution of the Hall gauge. From the energy-level scheme presented in Fig. 2, we know that five non-degenerate subsystems can be formed with the bias field.

Figure 6 plots the experimental results of the bluer gain peak split in the magnetic field. We can find that it is split into five peaks as expected. One locates at the line center corresponding to the non-magnetic field case, while the others are symmetrically distributed on two sides. When the magnetic

field increases, the frequency difference between two neighboring peaks is increased, which is proportional to the applied field with a coefficient of 0.934 MHz/G. The frequency difference between arbitrary two neighboring peaks is the same under the magnetic field. Figure 7 plots the redder gain peak split in the magnetic field. We can see that the redder gain peak is also split into five peaks, although it has litter dispersion. As the magnetic field increases, the shape of the five peaks becomes obvious. The frequency distance between the adjacent peaks is the same as the bluer one.

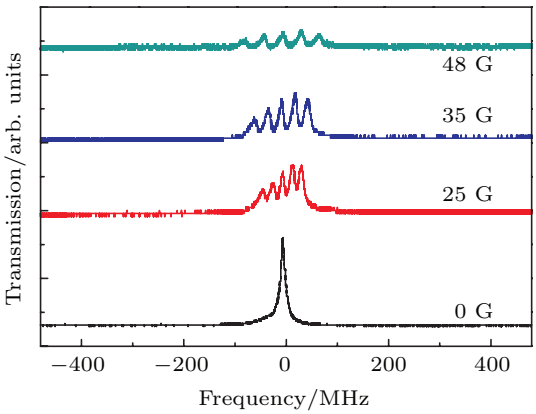


Fig. 6. (color online) Splitting of the bluer Raman gain in a longitudinal magnetic field. The colored curves show the splitting of Raman gain resonances with different magnetic fields.

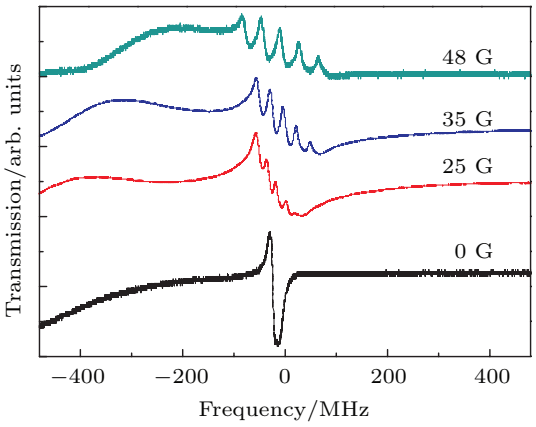


Fig. 7. (color online) Splitting of the redder Raman gain in a longitudinal magnetic field. The colored curves show the splitting of Raman gain resonances with different magnetic fields.

3.3. Multi Raman resonance with a transverse magnetic field

Next, we study the splitting of the Raman gain resonance in a transverse magnetic field. From Fig. 3, we know that six independent subsystems will be formed, each of which is shifted slightly from the line center. When the bias field is applied, six gain peaks will appear and form a symmetric structure.

Figure 8 plots the results of the bluer gain peak split in a transverse magnetic field. Since the transition strengths between different Zeeman levels are very different for the probe beam, we can see that it is split into six resonances with different intensities. The six peaks are symmetric to the resonance without the bias magnetic field. Figure 9 plots the results of the redder gain peak split in a magnetic field. As the redder gain peak locates near the Doppler absorption profile, the Raman gain is competed with the absorption. We can observe multi absorption resonances rather than multi Raman gain peaks when the transverse magnetic field is applied. We emphasize that the distance between the adjacent two peaks is the same as the bluer one, which agrees well with the theoretical calculation.

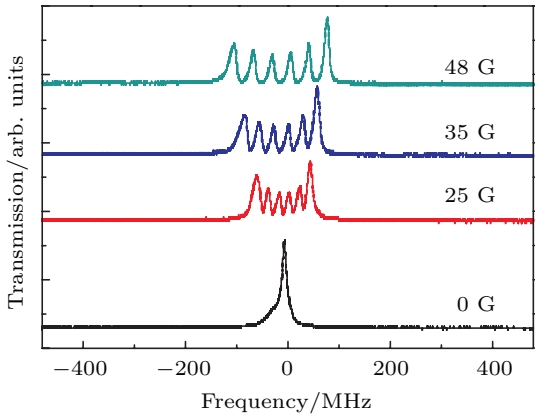


Fig. 8. (color online) Splitting of the bluer Raman gain in a transverse magnetic field. The colored curves show the splitting of Raman gain resonances with different magnetic fields.

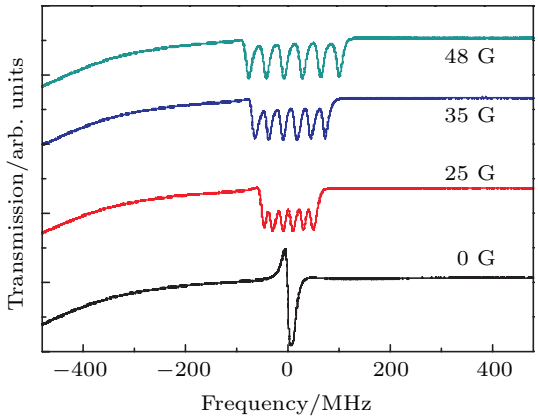


Fig. 9. (color online) Splitting of the redder Raman gain in a transverse magnetic field. The colored curves show the splitting of Raman gain resonances with different magnetic fields.

4. Conclusion

From these experimental results, we find that the Raman gain resonance for ^{85}Rb atoms can be split into five or six peaks when a bias magnetic field is applied. The frequencies of these multi-Raman gain resonances can be easily controlled by the magnetic field, which enables us to amplify the probe beam at different frequencies and generate the associated conjugate beams. With such multi gain resonances, the relative intensity squeezing between the probe and the conjugate beams can be generated based on this configuration at

different frequencies simultaneously. In principle, we can use a Fabry–Perot cavity or etalon to separate these different frequency components. Such a system can be used for multi-color correlated twin beams as well as for multi-channel quantum information processing.

In summary, we have experimentally investigated the multi Raman gain resonances in FWM process with ARG. Because two two-photon resonances are established in the double-Λ system, we can observe clearly the Raman gain resonances. When a bias magnetic field is applied, the system can form several subsystems due to the separated Zeeman levels. In the case of a longitudinal magnetic field, the Raman gain resonance splits into five peaks. When the magnetic field is applied transversely, six peaks can be observed. Based on the advantage of simplicity of the experimental realization, the results we have obtained have potential applications in the measurement of magnetic fields and the generation of multi-frequency correlated twin beams.

References

[1] Agarwal G S, Dey T N and Gauthier D J 2006 *Phys. Rev. A* **74** 043805
[2] Jiang K J, Deng L and Payne M G 2006 *Phys. Rev. A* **74** 041803
[3] Jiang Q C, Liu C, Liu J H and Zhang J X 2015 *Acta Phys. Sin.* **64** 094208 (in Chinese)
[4] Wang L J, Kuzmich A and Dogariu A 2000 *Nature* **406** 277
[5] Deng L and Payne M G 2007 *Phys. Rev. Lett.* **98** 253902
[6] Zhang L D, Jiang Y, Wan R G, Tian S C, Zhang B, Zhang X J, Gao J Y, Niu Y P and Gong S Q 2011 *J. Phys. B* **44** 135505
[7] McCormick C F, Boyer V, Arimondo E and Lett P D 2007 *Opt. Lett.* **32** 178
[8] Qin Z Z, Jing J T, Zhou J, Liu C J, Pooser R C, Zhou Z F and Zhang W P 2012 *Opt. Lett.* **37** 3141
[9] Yu X D, Meng Z M and Zhang J 2013 *Chin. Phys. B* **22** 094204
[10] Guo M J, Zhou H T, Wang D, Gao J R, Zhang J X and Zhu S Y 2014 *Phys. Rev. A* **89** 033813
[11] Wei D, Liu J, Yu Y, Wang J W, Gao H and Li F L 2015 *J. Phys. B* **48** 245401
[12] Zibrov A S, Ye C Y, Rostovtsev Y V, Matsko A B and Scully M O 2002 *Phys. Rev. A* **65** 043817
[13] Novikova I, Phillips D F, Zibrov A S, Walsworth R L, Taichenachev A V and Yudin V I 2006 *Opt. Lett.* **31** 2353
[14] Novikova I, Phillips D F, Zibrov A S, Walsworth R L, Taichenachev A V and Yudin V I 2006 *Opt. Lett.* **31** 622
[15] Hancox C, Hohensee M, Crescimanno M, Phillips D F and Walsworth R L 2008 *Opt. Lett.* **33** 1536
[16] Slavov D, Sargsyan A, Sarkisyan D, Mirzoyan R, Krasteva A, Wilson-Gordon A D and Cartaleva S 2014 *J. Phys. B* **47** 035001
[17] Sargsyan A, Mirzoyan R, Papoyan A and Sarkisyan D 2012 *Opt. Lett.* **37** 4871
[18] Steck D A 2013 *Rubidium 85 D line data* http://steck.us/alkalidata/
[19] Guo X, Zhao J and Li Y 2012 *Appl. Phys. Lett.* **100** 091112
[20] Gao H, Rosenberry M, Wang J and Batelaan H 2005 *J. Phys. B* **38** 1857